Journal of Alloys and Compounds 511 (2012) 45–49

Contents lists available at SciVerse ScienceDirect

Journal of Alloys and Compounds

journal homepage: www.elsevier.com/locate/jallcom

A novel fading-resistant Al–3Ti–3B grain refiner for Al–Si alloys

Tongmin Wang, Hongwang Fu, Zongning Chen*, Jun Xu, Jing Zhu, Fei Cao, Tingju Li

School of Materials Science and Engineering, Dalian University of Technology, Dalian 116024, PR China

ARTICLE INFO

Article history:
Received 11 May 2011
Received in revised form 15 August 2011
Accepted 4 September 2011
Available online 10 September 2011

Keywords:
Metals
Casting
Al–Ti–B master alloy
Grain refinement

ABSTRACT

Al–Ti–B refiners with excess-Ti perform adequately for wrought aluminum alloys but inefficiently in the case of foundry alloys. The high content of silicon in the latter, which forms silicides with Ti and severely impairs the refining potency of the nuclei, is known to be responsible for the poor performance. Hence, new grain refiners, such as Al–3B and Al–3Ti–3B master alloys with excess-B have been developed with well documented advantages for Al–Si alloys. It is very desirable to involve $TiAl_3$ particles in the Al–3Ti–3B master alloy to maximize its grain refining efficiency. However, fading phenomenon is a key drawback for application of the $TiAl_3$-containing refiners in aluminum foundry. In the present work, new Al–3Ti–3B grain refiners, containing TiB_2, AlB_{12} and $TiAl_3$ particles were developed with an aim to prolong the acting time after inoculation. The results showed that inoculation of Al–7Si alloy with thus meliorated Al–3Ti–3B grain refiner has produced a fine grain structure which was approximately maintained up to 30 min.

1. Introduction

Addition of grain refiner master alloys to molten aluminum produces fine, equiaxed grain structures which imparts to the castings high yield strength, high toughness, good extrudability, and uniform distribution of second phase and microporosity on a fine scale resulting in improved machinability [1–3]. Commercial refiners are manufactured from Al–Ti–B ternary system, usually with excess Ti in its composition than that required to form TiB_2 [4–7]. Hence, TiB_2 and $TiAl_3$ are the main phases except for the α-Al matrix in the master alloys. The former acts as potential nucleating site while $TiAl_3$ particles are readily dissolved in the melt to provide solute Ti, the participation of which can not only activate the nucleating potency of TiB_2, but also slows down the grain growth of α-Al during the solidification process [8,9].

But in the case of aluminum foundry alloys, in which the content of Si is typically higher than 2 wt.%, the efficiency of the popular Al–5Ti–B master alloy will be severely impaired. This is known as the poisoning effect resulted from the interaction between solute Ti and Si. To solve this problem, one effective method is to increase the addition level of Al–5Ti–B refiner, which is, however, expensive and undesirable in practice. Al–3B master alloy has been reported to be more effective during grain refining hypoeutectic Al–Si alloys [10]. This work was later confirmed by Sigworth et al. and a new Al–3Ti–3B refiner, in which $(Ti,Al)B_2$ and AlB_2 are the potent nucleating sites, has been developed with improved performances [11].

Among various methods to produce Al–Ti–B master alloys [12–20], that which involving the reaction between fluoride salts and molten aluminum, namely halide salt route, is the most popular [3]. Based on a large quantity of research focusing on improving the fabrication method for Al–Ti–B master alloys [21–27], Birol combined conventional halide salt route and powder metallurgy (PM) process into a new method which gave birth to a novel Al–3Ti–3B master alloy consisting of both $TiAl_3$ and AlB_2 particles on a fine scale [28]. The results in his work showed that this refiner is fast acting and more effective with respect to the Al–3B master alloy in refining Al–7Si alloy. Nevertheless, this refiner can be used only when casting is made shortly after inoculation since at prolonged holding time, transformation of AlB_2 to TiB_2 is unavoidable. On the other hand, it is very desirable to replace the PM procedure in the process, from technical and economical reasons, with a simple halide salt route.

The present work was undertaken to develop the conventional halide salt route to produce an Al–3Ti–3B alloy containing $TiAl_3$ particles. The sluggish peritectic reaction of AlB_{12} to AlB_2 in liquid aluminum was used to stabilize $TiAl_3$ particles in an excess-B concentration and to prolong the effective time during holding after inoculation.

2. Experimental procedure

Al–3Ti–3B master alloys were synthesized in the laboratory via the halide salt route with modified steps: Al–6Ti and Al–6B master alloy were primarily prepared separately and then mixed together in order to keep the unreacted aluminides and borides from transforming into TiB_2.

* Corresponding author at: School of Materials Science and Engineering, Dalian University of Technology, No.2 Linggong Road, Ganjingzi District, Dalian City, Liaoning Province, PR China. Tel.: +86 041184706790; fax: +86 041184706790.
E-mail address: diffen1986@163.com (Z. Chen).

0925-8388/$ – see front matter © 2011 Elsevier B.V. All rights reserved.
doi:10.1016/j.jallcom.2011.09.009

Table 1
Status of the experimental refiners used in this work.

Alloy no.	Composition (wt.)		Synthesis temperature (°C)	Synthesis practice	Holding time (min)	Particle type
	Ti%	B%				
1	0	3	750	Cast	–	AlB_2
2	0	3	950	Cast	–	$AlB_2 + AlB_{12}$
3	3	3	800 + 1000	Mixed	0	$TiAl_3 + TiB_2 + AlB_{12}$
4	3	3	800 + 1000	Mixed	5	$TiAl_3 + TiB_2 + AlB_{12}$
5	3	3	800 + 1000	Mixed	30	$TiAl_3 + TiB_2 + AlB_{12}$

Al–6Ti master alloy was produced by reacting K_2TiF_6 salt with molten aluminum on a 150 g batch scale. The primary materials were pure aluminum (99.7% Al) and K_2TiF_6 powder (commercial purity). Aluminum ingot was firstly cut and heated to a required temperature in a graphite crucible using a medium-frequency induction furnace to facilitate a rapid melting. The molten metal thus obtained was transferred into a resistance furnace to hold the melt isothermally at 800 °C. K_2TiF_6 salt, weighed to achieve a composition of Al–6Ti in the alloy, was compacted to a cylindrical block and added into the aluminum melt without introducing any stirring. The experimental Al–6B master alloy was produced under the same conditions except for the different addition temperature which was 1000 °C to promote the formation of AlB_{12} phase. The molten alloys were held at the addition temperature for 30 min. Subsequently, the melts were stirred with a graphite rod for 30 s and mixed thoroughly after decanting the by-product K–Al–F salt from its surface. The mixed alloys were finally cast into a water-cooled copper mold after different holding times, i.e. 0, 5 and 30 min, respectively. Samples were sectioned from the final alloys and then prepared with standard metallographic procedure. The microstructures of the samples were characterized under MEF4A optical microscope after etching with Busswell's reagent. Phases were identified using XRD analysis.

For grain refinement study of each refiner, 400 g Al–7Si alloy was melted in a graphite crucible using the medium-frequency induction furnace and then transferred into a mini resistance furnace to maintain the temperature of the melt within 700 ± 10 °C in the whole procedure. Both the experimental Al–3Ti–3B alloys and the AlB_2-, AlB_{12}-type Al–3B alloys have been tested to recognize the most efficient grain refiner. A reference sample was taken from the melt with an aim to identify the grain size before inoculation. 0.67 g of the experimental master alloy was then inoculated into the melt. This is the exact amount of an Al–3Ti–3B or Al–3B master alloy needed to bring the B concentration of 400 g aluminum melt to 0.005 wt.%. The melt was stirred with a graphite rod for 30 s as soon as the inoculation completed. Samples were taken from the melt 2, 10, 30 and 60 min respectively after the inoculation and casted into a steel mold with a diameter of 25 mm and a height of 45 mm. The samples thus produced were sectioned 20 mm from the bottom and then ground using SiC paper up to 1000 mesh. Standard polishing procedure was employed and these samples were then etched with Poulton's reagent to highlight the grain boundaries. The mean linear intercept was then estimated by counting the number of grain-boundary intercepts along two perpendicular 8 mm long lines. Eight different locations were measured for each sample surface and an average grain size was reported.

3. Results and discussion

Table 1 is the status of the experimental refiners used in this work. The AlB_2- and AlB_{12}-type Al–3B master alloys (alloy 1 and 2), as reference refiners to investigate the impact of different nucleating particles on refinement, were synthesized under different processing techniques. Formation of AlB_2 and AlB_{12} is expected to proceed in terms of Reactions (1) and (2), respectively. Busswell's reagent provides a simple route to distinguish the borides in an Al–B alloy under an optical microscope. Diborides, TiB_2 and AlB_2, are capable of being colored with copper while AlB_{12} is not [29,30]. Alloy 1 is a conventional Al–3B master alloy in which AlB_2 particles are light brown and less than 20 μm (Fig. 1a). Alloy 2, which is actually a mixture of AlB_2 and AlB_{12} in α-Al matrix, was synthesized under a modified halide salt route to fulfill its destiny. Detailed manufacturing procedures can be found in the literature [31]. The AlB_2 in alloy 2 exhibits two types of morphologies. Unlike the blocky particles in alloy 1, the vast majority of AlB_2 particles in alloy 2 are strip-like. This is attributed to the supersaturation of solute B resulted from cooling of the alloy, leading to the precipitation of AlB_2 at the grain boundary. The other type of AlB_2, although relatively less in numbers, can be seen as regular hexagonal plate. AlB_{12} particles, on the other hand, are gray and of irregular morphologies (Fig. 1b). Fig. 3a and b show the XRD patterns obtained from the Al–3B master alloys. It clearly reveals the presence of AlB_2, AlB_{12} and α-Al phases. Some unidentified peaks are suggested to be the spent K–Al–F salts. The reactions from which the two kinds of boride particles are formed were reported to be [32]:

$$2KBF_4 + 3Al = AlB_2 + 2KAlF_4 \quad (1)$$

$$12KBF_4 + 13Al = AlB_{12} + 12KAlF_4 \quad (2)$$

Our previous work has confirmed grain refining potency of Al–B master alloy on pure aluminum. AlB_2 particles are, but less efficient nucleating sites for Al grains in refining commercial pure aluminum. Thanks to the sluggish transformation of AlB_{12} to AlB_2 in aluminum melt, AlB_{12} is of great help to overcome the fading during holding after inoculation [31]. Further studies of this on grain refinement of Al–7Si alloy have been performed in the present work. The results were similar to that on 99.7% pure aluminum. An adequate fine grain structure was obtained within 2 min of inoculation at a modest 0.005 wt.% addition level. Fading of the refinement

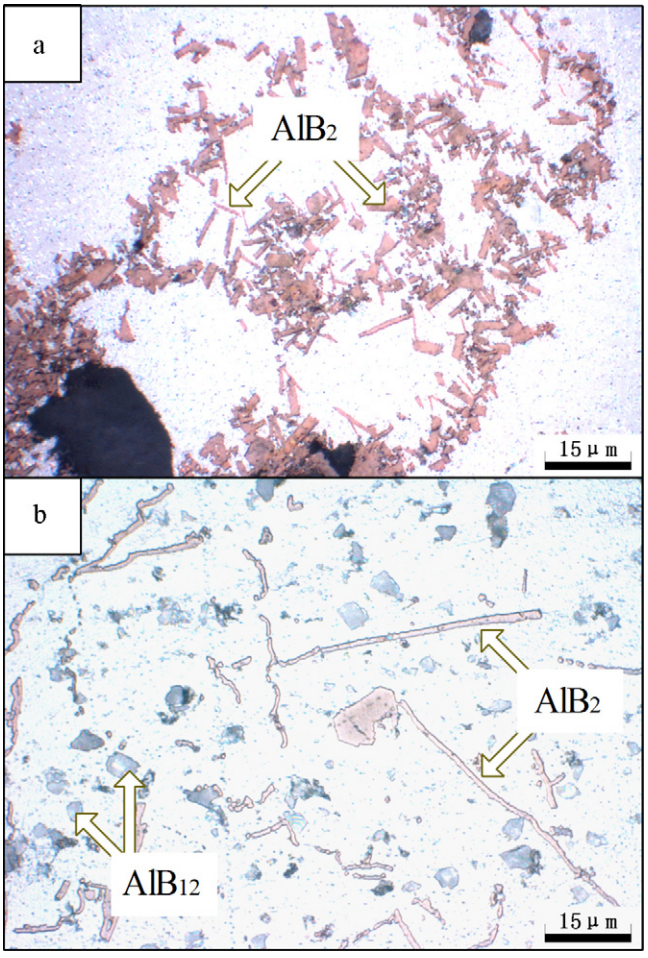

Fig. 1. Microstructural features of the experimental Al–3B grain refiner alloys with different temperatures: (a) 750 °C (alloy 1), (b) 950 °C (alloy 2).

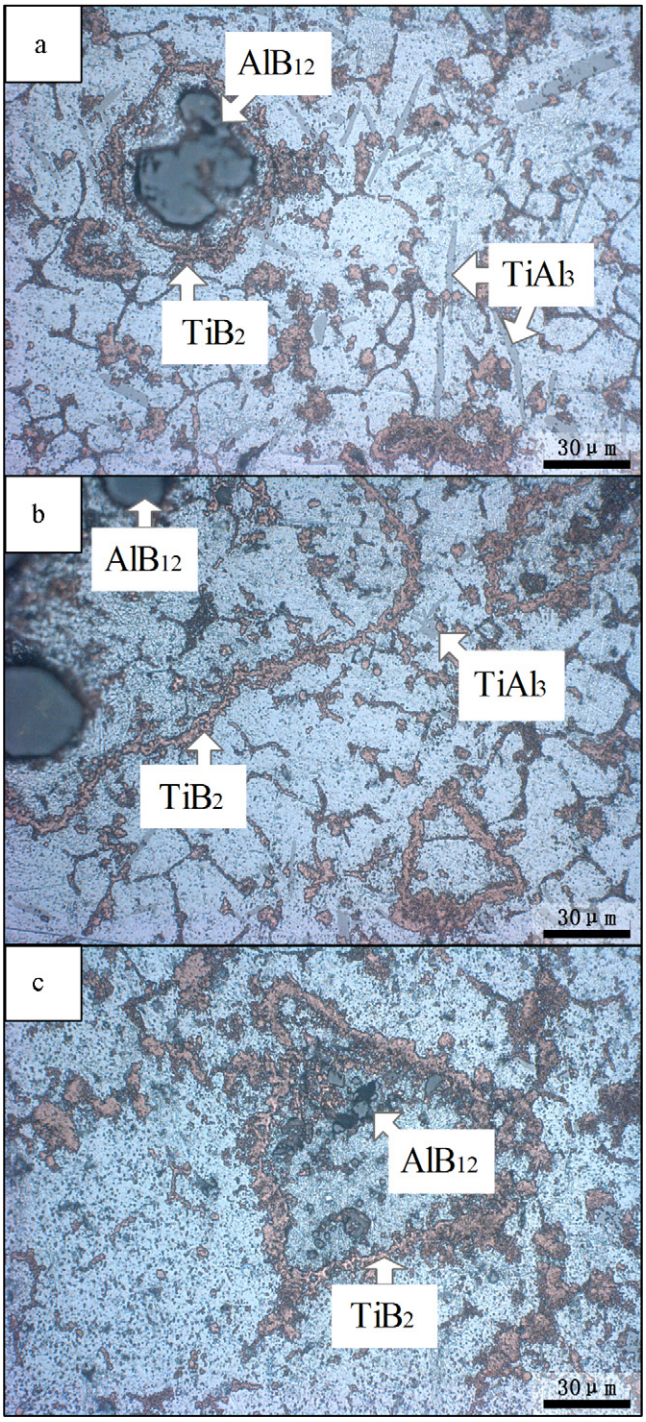

Fig. 2. Microstructural features of the experimental Al–3Ti–3B grain refiner alloys with different holding times: (a) 0 min (alloy 3), (b) 5 min (alloy 4) and (c) 30 min (alloy 5).

effect for the two alloys, however, was different. Complete loss of grain refinement was found in the sample of 60 min holding after inoculation with alloy 1. Dissolution of AlB_2 in the inoculated melt is responsible for the fading. Alloy 2, the AlB_{12}-type refiner, profits from the presence of AlB_{12} and the effective time of refinement was thus prolonged. The grain refining efficiency was somehow retained after 60 min holding of the melt.

The Al–3Ti–3B master alloy, cast shortly after mixing (alloy 3), is a homogeneous mixture of α-Al grains with a dispersion of three types of particles (Fig. 2a). XRD pattern of this alloy clearly shows

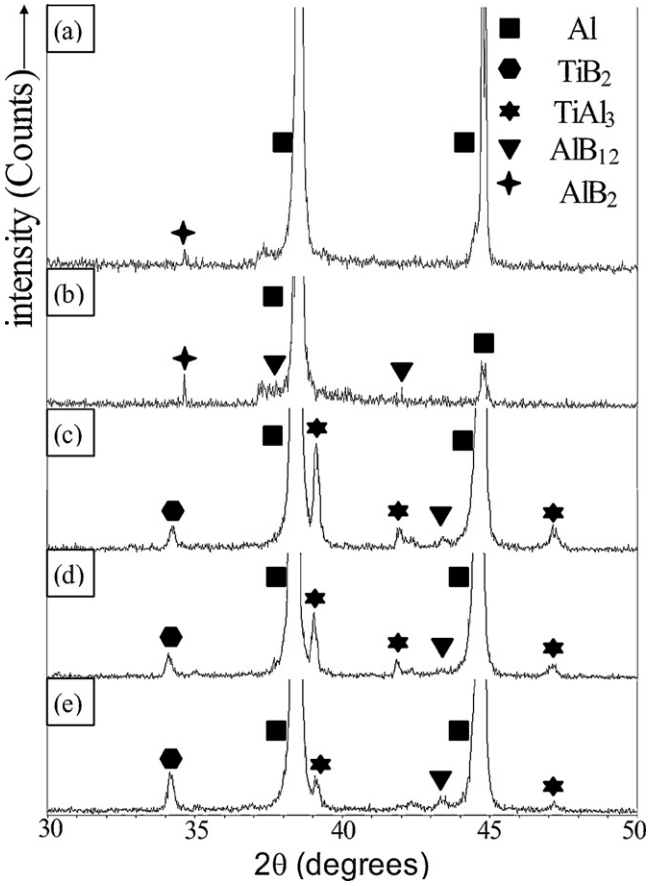

Fig. 3. XRD patterns of the master alloys used in this work: (a) alloy 1, (b) alloy 2, (c) alloy 3, (d) alloy 4 and (e) alloy 5.

that these particles comprised TiB_2, $TiAl_3$ and AlB_{12} (Fig. 3c). The three particles formed according to Reactions (1)–(3) [28,32]:

$$3K_2TiF_6 + Al + 3AlB_2 = 3TiB_2 + 3KAlF_4 + K_3AlF_6 \quad (3)$$

The three particles can be identified readily from the optical micrographs after etching with Busswell's reagent. $TiAl_3$ and AlB_{12} can be distinguished by their different colors and morphologies. $TiAl_3$ particles, seen as light gray, are predominantly flaky and approximately 30 μm. Several petal-like $TiAl_3$ particles were also noted in Fig. 1a.(For interpretation of the references to color in this text, the reader is referred to the web version of the article.) These observations are consistent with those of Arnberg et al. [33] who have shown that flaky and petal-like $TiAl_3$ particles dominated at high temperatures. Wang et al. [34] pointed out that the morphology of $TiAl_3$ would be affected by other elements such as B, Li and Mg. In this work, the morphology of $TiAl_3$ particles may be attributed to both of the two reasons. AlB_{12}, seen as huge lumps from Fig. 2a, is dark gray and invariably surrounded by finer particles. Recalling that TiB_2 can be colored by copper after etching with Busswell's reagent, it is fair to infer that the fine, light brown particles in Fig. 2a are TiB_2 aggregation. (For interpretation of the references to color in this text, the reader is referred to the web version of the article.)

It is also noted from Fig. 2a that, in the Al–3Ti–3B master alloys, large AlB_{12} lumps are always surrounded by chain-like TiB_2 particles. Similar features are also exhibited in the microstructure of alloy 4 and 5 (Fig. 2b and c). However, as the holding time was prolonged, AlB_{12} became smaller inside the TiB_2 particle rings. When the melt was held for 30 min before casting, the large AlB_{12} lumps were fractured into small pieces and $TiAl_3$ particles can be hardly seen in the microstructure of the final alloy (Fig. 2c). From the

above all, we can conclude that AlB_{12} and $TiAl_3$ may take reactions to form TiB_2. In fact, the microstructures of the Al–3Ti–3B master alloys with different holding times revealed the formation mechanism of TiB_2 in this alloy. Considering that the Al–3Ti–3B master alloy is a B-excess one, TiB_2 should have agglomerated in the interface between the $TiAl_3$ particles and matrix according to Emamy's model [35]. However, the results were in disagreement with the views of the above. This is mainly attributed to that the borides in the experimental Al–6B master alloy, due to the high synthesis temperature, were predominantly AlB_{12}. Owing to the sluggish peritectic reaction of AlB_{12} in aluminum melt, no sufficient solute boron atoms were capable of being supplied aside the $TiAl_3$ surface for the following reaction between Ti and B. Instead of that, solute titanium was in excess and TiB_2 would be agglomerated in the B-enriched area near the AlB_{12} surface. Anyhow, AlB_{12} dissolved gradually, leading to the observations of fragments in Fig. 2b and small pieces in Fig. 2c inside the agglomerated TiB_2 rings. The sluggish peritectic reaction is also evidenced by the still existing AlB_{12} particles in the final alloy up to holding of 30 min.

$$AlB_{12} + 6[Ti] = Al + 6TiB_2 \quad (4)$$

Formation of TiB_2 in the experimental Al–3Ti–3B alloy can be drawn as Reaction (4). The gradual dissolving of AlB_{12} and formation of TiB_2 illustrated above are demonstrated from the XRD spectra of the experimental alloys (Fig. 3c–e). The most intensified signals in the XRD patterns, except for that of α-Al, are of TiB_2, $TiAl_3$ and AlB_{12} varieties. Remarkable increase in the fraction of the TiB_2 variety and decreases in the fraction of $TiAl_3$ and AlB_{12} variety can be seen from Fig. 3c–e when the holding time was increased. Besides, lack of the signals of the by-product K–Al–F salts in the XRD reflections indicates that the residual salt, always introduced when the PM process is involved, was almost removed out from the melt after decanting. The by-product K–Al–F salts, originated from the halide salt reactions according to Eqs. (1)–(3). It has been reported that the efficiency of Al–Ti–B refiners are strongly influenced by the spent salts in the final alloys [36]. It is thus claimed that involvement of spent salts, which the PM process inevitably suffers, can be overcome adequately by the present process for producing Al–3Ti–3B master alloys containing $TiAl_3$ particles.

Distribution of the TiB_2 particles in α-Al matrix of the master alloys was noted in terms of the different holding times. In the case of 30 min holding (alloy 5), more TiB_2 particles were dispersed inside the α-Al grains and very few were found as clusters at the grain boundaries (Fig. 2c). Solute Ti, consumed gradually by the reaction to form TiB_2 during holding, played an important role in the dispersion of TiB_2 particles. Although the Al–3Ti–3B alloy was in deficient in Ti, as a result of the sluggish peritectic reaction, the majority of boron atoms would be locked in the AlB_{12} box for a while after mixing of the two molten alloys. Hence, at the earlier stage after mixing, Ti was yet the dominant solute in the mixed molten alloy. It has been confirmed in the literature that in a Ti-rich Al–Ti–B alloy, TiB_2 acts as a substrate for the formation of $TiAl_3$ during solidification [37,38]. Consequently, TiB_2 clusters would be embedded in the sheath of $TiAl_3$. These accounts for the chain-like TiB_2 agglomerates observed in the microstructures of alloy 3 and 4 (Fig. 2a and b). The gradual dispersion of TiB_2 after long holding time is an indirect evidence for the fact that after mixing of the Al–Ti and AlB_{12}-type Al–B master alloy, the melt will be rich in solute Ti and therefore $TiAl_3$ can be stabilized by the presence of AlB_{12}. Alloy 3, in which numerous $TiAl_3$ particles were present, exhibited favorable features and thus performed best in the grain refinement test on Al–7Si alloy (Fig. 4). Grain structure of the Al–7Si alloy enjoys the contribution of $TiAl_3$ particles such that alloy 3 was found to be a fast acting refiner. Inoculation with alloy 3 has produced a fine and equiaxed grain structure across the entire section of the test sample 2 min after inoculation and the efficacy was

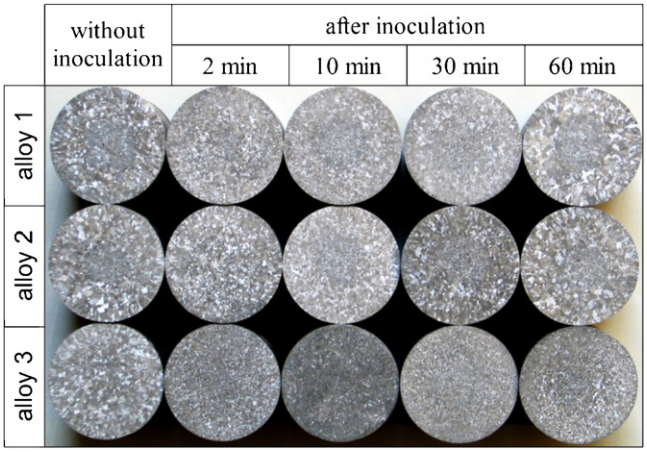

Fig. 4. Grain refinement tests of the experimental Al–3Ti–3B refiner on Al–7Si alloy with respect to the two Al–3B refiners.

almost completely retained for as long as 30 min holding. The fast acting feature of the refiner is attributed to the presence of $TiAl_3$ which is known to be an efficient nucleating site for α-Al grains. Fading of the refining effect after 30 min holding of the inoculated melt, is superior to the Al–3Ti–3B refiner fabricated by PM route could offer, i.e. a notable fading at holding times longer than 15 min [28]. This may be linked with the modest particle size of $TiAl_3$ in the master alloy produced by the present process. $TiAl_3$ particles fabricated by reaction of K_2TiF_6 and Al in solid state are in such a fine scale that dissolving can proceed more rapidly. The dissolved Ti may form silicides with Si and/or form TiB_2 with boron, both of which will strongly impair the grain refining performance. Given prolonged holding times, the sluggish peritectic transformation of AlB_{12} to AlB_2, which is an alternative potent nucleating site for α-Al grain, is also responsible for the fading-resistant feature of the refiner [31].

Alloys 4 and 5 were designated to investigate the effect of transformation of AlB_{12} and $TiAl_3$ into TiB_2 on the performance of the Al–3Ti–3B refiner. Lacking of $TiAl_3$ and AlB_{12} resulted in inferior performances of the two alloys in spite of the more uniform distribution of TiB_2 in alloy 5 (Fig. 5). This is not astonishing since TiB_2 is known to be as less efficient nucleating site for hypoeutectic Al–Si alloys. The grain structures of the 2 min samples inoculated with alloy 4 and 5 are quite similar to that with the AlB_{12}-type alloy 2. This confirms the important impact of $TiAl_3$ on the refiner to obtain an outstanding refining efficiency.

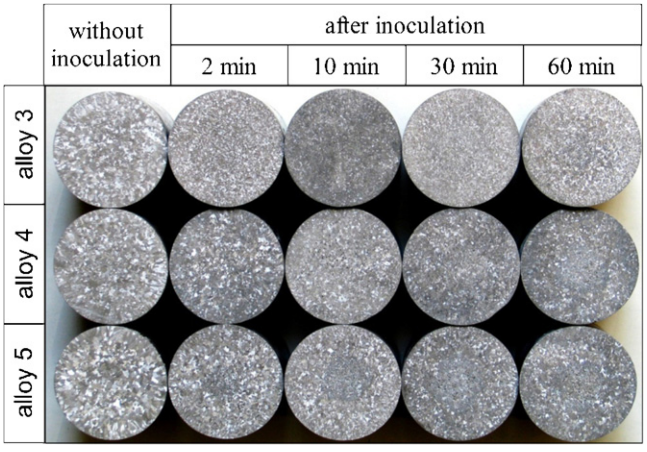

Fig. 5. Grain refinement tests of the Al–3Ti–3B grain refiners with different holding times on Al–7Si alloy.

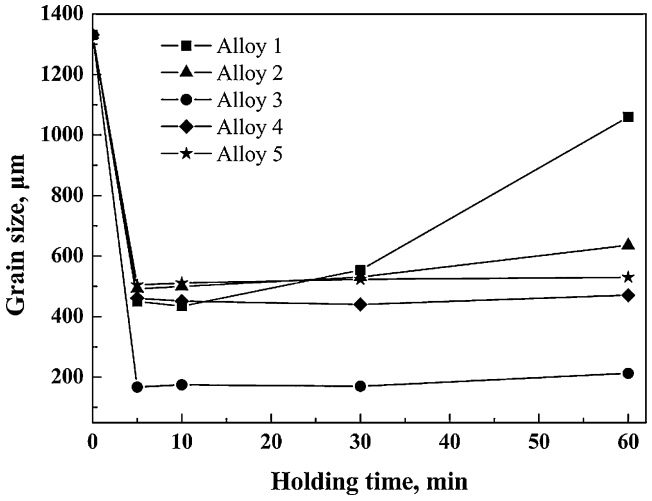

Fig. 6. The average grain size of the samples with different holding times after inoculation of alloys 1–5.

To illustrate the better performance of alloy 3, Fig. 6 shows the quantitative average grain size analysis. It could be clearly seen that alloy 2–5, in which AlB_{12} existed, all exhibited resistance to fading after long period of holding time. While alloy 1, in which AlB_2 is the predominated phase, was found so easy to lose its grain refining efficiency that complete failure of grain refinement occurred in the sample 60 min after inoculation. From the grain analysis, 2 min after inoculation of alloy 3 has produced a fine equiaxed grain structure (167 μm) which was almost entirely retained for 30 min. This grain refinement is much superior to that inoculated with the binary Al–3B alloy (435 μm for the sample 2 min after inoculation) in this work. The reduction in grain size is remarkable in spite of the modest addition level of 0.005% B (or Ti). It confirms the favorable contribution of $TiAl_3$ on the grain refinement of Al–7Si alloy [28]. So, it is inferred from the foregoing observations that casting of the master alloy shortly after mixing produces the best, fast acting and fading-resistant Al–3Ti–3B refiner for Al–Si alloys.

4. Conclusions

By mixing separately synthesized Al–Ti and Al–B master alloys, a novel Al–3Ti–3B grain refiner, in which TiB_2, $TiAl_3$ and AlB_{12} particles dispersed, has been produced in this work. The final products yielded a superior grain refining performance with respect to the Al–3B master alloys. AlB_{12} plays an important role for the improved performances in grain refinement. During fabrication of the Al–3Ti–3B master alloy, increased holding time after mixing contributes to the reaction between AlB_{12} and $TiAl_3$, which severely impairs the refining efficiency of the final products. Hence, it is required to cast the Al–3Ti–3B master alloy shortly after mixing of the two melts in order to obtain a good grain refining performance.

The present study provided a new grain refiner for Al–Si foundry alloys. It can be used in the casting of aluminum alloys, especially when a long holding time of grain refining efficiency is required. Meanwhile, the results have shown that Al–Si alloys can enjoy grains as small as those of the wrought alloys, well below 200 μm, with an addition of only 0.005 wt.%B. This offers many technical benefits for the casting of Al–Si alloys.

Acknowledgements

Authors would like to thank National Natural Science Foundation of China (Nos 50601003, 50971032, 50874022), Scientific Research Fund of Liaoning Provincial Education Department, and Liaoning BaiQianWan Talents Program.

References

[1] A. Ohno, I. Motege, Solidification Technology in the Foundry and Casthouse, The Metals Society, London, 1983, 171–175.
[2] A. Hardman, F.H. Hayes, Mater. Sci. Forum 217–222 (1996) 247–252.
[3] B.S. Murty, S.A. Kori, M. Chakraborty, Int. Mater. Rev. 47 (2002) 1–29.
[4] C.D. Mayes, D.G. McCartney, G.J. Tatlock, Mater. Sci. Technol. 9 (1993) 97–103.
[5] A. Hardman, F.H. Hayes, Mater. Sci. Forum 247 (1996) 217–222.
[6] G.P. Jones, J. Pearson, Metall. Trans. 7B (1976) 223–234.
[7] M.S. Lee, B.S. Terry, Mater. Sci. Technol. 7 (1991) 608–612.
[8] M.A. Easton, D.H. StJohn, Metall. Mater. Trans. 30A (1999) 1613–1623.
[9] P. Schumacher, A.L. Greer, J. Worth, P.V. Evans, M.A. Kearns, P. Fisher, A.H. Green, Mater. Sci. Technol. 14 (1998) 394–404.
[10] H.T. Wu, L.C. Wang, S.K. Kung, J. Chin, Foundryman's Assoc. 29 (1981) 10–18.
[11] G.K. Sigworth, M.M. Guzowaski, AFS Trans. 93 (1985) 907–912.
[12] Q. Zhuxian, Y. Yaxin, Z. Mingjie, S.K. Grotheim, H. Kvande, Aluminium 64 (1988) 606–609.
[13] I.G. Davies, J.M. Dennis, A. Hellawell, Metall. Trans. 1 (1970) 275–280.
[14] I. Maxwell, A. Hellawell, Acta Metall. 23 (1975) 895–899.
[15] J. Kaneko, M. Sugamata, R. Shimamune, S. Seshan, Trans. Jpn. Foundrymen's Soc. 10 (1991) 72–75.
[16] M.G. Chu, Mater. Sci. Eng. A 179–180 (1994) 669–675.
[17] D.G. McCartney, Int. Mater. Rev. 34 (1989) 247–260.
[18] B.S. Murty, S.A. Kori, K. Venkateswarlu, R.R. Bhat, M. Chakraborty, J. Mater. Process. Technol. 89–90 (1999) 152–158.
[19] M.S. Lee, B.S. Terry, P. Grieveson, Metall. Trans. B 24B (1993) 947–953.
[20] M.J. Jackson, I.D. Graham, J. Mater. Sci. Lett. 13 (1994) 754–756.
[21] Y. Birol, J. Alloys Compd. 420 (2006) 71–76.
[22] Y. Birol, J. Alloys Compd. 420 (2006) 207–212.
[23] Y. Birol, J. Alloys Compd. 427 (2007) 142–147.
[24] Y. Birol, J. Alloys Compd. 440 (2007) 108–112.
[25] Y. Birol, J. Alloys Compd. 443 (2007) 94–98.
[26] Y. Birol, J. Alloys Compd. 478 (2009) 265–268.
[27] Y. Birol, J. Alloys Compd. 480 (2009) 311–314.
[28] Y. Birol, J. Alloys Compd. 486 (2009) 219–222.
[29] N. El-Mahallawy, M.A. Taha, A.E.W. Jarfors, H. Fredriksson, J. Alloys Compd. 292 (1999) 221–229.
[30] J. Fjellstedt, A.E.W. Jarfors, Mater. Sci. Eng. A 413–414 (2005) 527–532.
[31] T.M. Wang, Z.N. Chen, H.W. Fu, J. Xun, Y. Fu, T.J. Li, Scripta Mater. 64 (2011) 1121–1124.
[32] X.M. Wang, J. Alloys Compd. 403 (2005) 283–287.
[33] L. Arnberg, L. Backerud, H. Klang, Met. Technol. 9 (1982) 1–6.
[34] X.M. Wang, A. Jha, R. Brydson, Mater. Sci. Eng. A 364 (2004) 339–345.
[35] M. Emamy, M. Mahta, J. Rasizadeh, Compos. Sci. Technol. 66 (2006) 1063–1066.
[36] Y. Birol, J. Alloys Compd. 458 (2008) 271–276.
[37] P.S. Mohanty, J.E. Gruzleski, Acta Metall. Mater. 43 (1995) 2001–2012.
[38] N. Iqbal, N.H. Van Dijik, S.E. Offerman, M.P. Moret, L. Katgerman, G.J. Kearley, Acta Mater. 53 (2005) 2875–2880.